Los Alamos
NATIONAL LABORATORY
memorandum
The Applied Theoretical Physics Division
XTM: Transport Methods Group

To/MS: Distribution

From/MS: A. Adams, S. Frankle, R. Little
Phone/FAX: 5-6461 / 5-5538
Symbol: XTM-RN(U)96-031
Date: December 24, 1996

Revised Criticality Benchmarks for MCNP

I. INTRODUCTION

The continuous-energy neutron data library ENDF60 for use with MCNP™ was released in the fall of 1994, and was based on ENDF/B-VI evaluations through Release 2.[1-3] As part of the data testing process for this library, a number of benchmark calculations were performed. A set of nine criticality benchmarks, a set of Lawrence Livermore National Laboratory (LLNL) Pulsed Sphere measurements, and a few shielding benchmarks, originally described in Los Alamos National Laboratory (LANL) report LA-12212,[4] were repeated for both ENDF/B-V and ENDF/B-VI based data. Upon further review, several errors were uncovered in the criticality benchmarks, prompting a comprehensive review of the set of nine benchmarks and expansion to include other criticality benchmarks.[5] Some preliminary results from this review have been published elsewhere.[6] Additionally, a review of the benchmarks based on the LLNL Pulsed Sphere measurements was also conducted and additional benchmarks implemented. The results of the LLNL Pulsed Sphere benchmark review have been documented elsewhere,[7] and a more comprehensive document will be produced. A review of the shielding benchmarks has not been performed but is planned for the future.

Section II of this report documents the revisions made to the original nine criticality benchmarks; Section III describes the additional benchmarks which have been implemented. In addition to original publications, two compendiums of experimental benchmarks were used extensively during this review: the Cross Section Evaluation Working Group (CSEWG)[8] and the International Criticality Safety Benchmark Evaluation Project (ICSBEP).[9] While the CSEWG specifications include descriptions of a number of additional measurements for each experiment, the ICSBEP specifications give a more complete physical description of the actual experiments but only focus on the calculation of k_{eff}. In addition to the standard k_{eff} calculation, we will also discuss other experimental information that can be evaluated with these benchmarks, and we give results from Godiva in Section IV. In Section V the work that has been performed to date will be summarized, and future work will be discussed.

Throughout this report, the following nomenclature will be used for referencing the vari-

ous data libraries which were used in this work:

ENDF/B-V ZAIDs ending in '.50c', or '.55c' for Fe, W, and ^{239}Pu
ENDF/B-VI ZAIDs ending in '.60c'

Data from the ENDL92 library, having a ZAID ending of '.42c', were used for natural tin (Sn), argon (Ar), and zinc (Zn).[10] Most of the major isotopes of interest to the criticality community were re-evaluated for ENDF/B-VI (^{1}H, ^{16}O, ^{235,238}U and ^{239,240,241}Pu). However, the evaluations for ^{232}Th, ^{233,234}U and ^{242}Pu are simply translations from ENDF/B-V, and differences in the results will be due to processing only. Photon production data has been added to the ^{233}U evaluation. Contributions from ^{2}H, ^{17}O and ^{18}O were not included for materials containing light water, as calculations performed showed that these contributions were negligible. The results reported in this research note were obtained using MCNP version 4xr on HP-735 computers. The values of k_{eff} quoted are from the combined estimator, and all calculated uncertainties listed are estimated statistical uncertainties at the 1σ level. This suite of criticality benchmarks will be archived on CFS, and we will consider making them available on the group's WWW server if there is sufficient interest.

II. REVISED BENCHMARKS FROM LA-12212

The original set of nine criticality benchmarks from LA-12212 is listed in Table 2 along with a fairly complete list of references for each benchmark. Each of these benchmarks will be discussed in turn.

Table 2: Criticality Benchmarks from LA-12212

Benchmark Name	References
Godiva*	8, 9, 11-14
Jezebel (4.5%)*	8, 9, 11-14
Jezebel (20.1%)*	8, 9, 11-14
Uranium Cylinder (10.9%)*	13, 15
Uranium Cylinder (14.11%)*	13, 15
Graphite Tamped Uranium Sphere	15
Water-Reflected Uranium Sphere	16
Three Uranium Cylinders*	17, 18
3x3 Pu Fuel Rod Array*	19

An * indicates that the benchmark has been revised from LA-12212.

A. Godiva Benchmark

The Godiva and Jezebel critical assemblies have been documented extensively. The Godiva benchmark is generally modeled as a simple sphere of highly enriched uranium (HEU). The material specifications for the Godiva benchmark have been modified from those given in LA-12212. ICSBEP developed several models for Godiva (referenced as HEU-MET-FAST-001); a simple sphere, nested spherical shells, and a slumped-shell model. We have implemented three models of Godiva; the CSEWG simple sphere model (referenced as F5), and the ICSBEP simple-sphere and nested spherical shell models. Table 3.a shows a comparison of the specifications for the simple-sphere model from LA-12212 with the CSEWG and ICSBEP simple sphere specifications. The results from the MCNP simulations are listed in Table 3.b, and these can be compared to the benchmark value of 1.000 ± 0.001.

Table 3.a: Specifications for Godiva

Nuclide	Atomic Density [#/barn-cm]		
	LA-12212 (R = 8.741 cm)	CSEWG F5 (R = 8.741 cm)	ICSBEP HEU-MET-FAST-001 (R = 8.7407 cm)
^{234}U	4.8943e-04	4.9200e-04	4.9184e-04
^{235}U	4.4966e-02	4.5000e-02	4.4994e-02
^{238}U	2.5287e-03	2.4980e-03	2.4984e-03

Table 3.b: MCNP Results for k_{eff} of Godiva

	ENDF/B-V	ENDF/B-VI
CSEWG: F5	0.9993 ± 0.0006	0.9977 ± 0.0006
HEU-MET-FAST-001: Simple Sphere	0.9966 ± 0.0007	0.9957 ± 0.0007
HEU-MET-FAST-001: Nested Spherical Shells	0.9972 ± 0.0007	0.9970 ± 0.0007

B. Jezebel Benchmarks

The Jezebel benchmarks consist of spheres of nickel-clad plutonium metal with 4.5 wt. % ^{240}Pu or 20.1 wt. % ^{240}Pu respectively. The material specifications for these benchmarks were not correct in LA-12212, and they have been revised to reflect either the CSEWG or ICSBEP specifications as listed in Tables 4.a and 5.a respectively. The Jezebel(4.5%) and Jezebel(20.1%) benchmarks are designated as CSEWG: F1 and F21, and ICSBEP:PU-MET-FAST-001 and -002 respectively. The results from the MCNP simulations are given in Tables 4.b and 5.b for Jezebel (4.5%) and Jezebel (20.1%) respectively. The benchmark value of k_{eff} is 1.000 ± 0.002 for each assembly.

Table 4a: Specifications for Jezebel (4.5%)

Nuclide	Atomic Density [#/barn-cm]		
	LA-12212 (R = 6.385 cm)	CSEWG: F1 (R = 6.3849 cm)	PU-MET-FAST-001 (R = 6.38493 cm)
^{239}Pu	3.7547e-02	3.7050e-02	3.7047e-02
^{240}Pu	1.7692e-03	1.7510e-03	1.7512e-03
^{241}Pu	0.0	1.1700e-04	1.1674e-04
Ga	0.0	1.3750e-03	1.3752e-03

Table 4.b: MCNP Results for k_{eff} of Jezebel (4.5%)

	ENDF/B-V	ENDF/B-VI
CSEWG: F1	1.0058 ± 0.0009	0.9978 ± 0.0009
PU-MET-FAST-001	1.0062 ± 0.0008	0.9974 ± 0.0009

Table 5a: Specifications for Jezebel (20.1%)

Nuclide	Atomic Density [#/barn-cm]		
	LA-12212 (R = 6.660 cm)	CSEWG: F21 (R = 6.6595 cm)	PU-MET-FAST-002 (R = 6.6595 cm)
^{239}Pu	3.1701e-02	2.9946e-02	2.9934e-02
^{240}Pu	7.8921e-03	7.8870e-03	7.8754e-03
^{241}Pu	0.0	1.2030e-03	1.2146e-03
^{242}Pu	0.0	1.4500e-04	1.5672e-04
Ga	0.0	1.3720e-03	1.3722e-03

Table 5.b: MCNP Results for k_{eff} of Jezebel (20.1%)

	ENDF/B-V	ENDF/B-VI
CSEWG: F21	1.0050 ± 0.0008	0.9994 ± 0.0009
PU-MET-FAST-002	1.0064 ± 0.0009	0.9986 ± 0.0007

C. Low Enriched Uranium Benchmarks

There were two low enrichment benchmarks specified in LA-12212, Uranium Cylinder (10.9%) and (14.11%), which have been designated as Low-1 and Low-3 for this report. The material specifications for both systems have been revised, and the remaining two systems, Low-2 (12.32%) and Low-4 (16.01%), have also been modeled and are discussed in the following section. These assemblies were actually layered plates of enriched ^{235}U, U(93.3%), and natural uranium, U(N), which have been homogenized for the MCNP problems. The specifications for the ^{234}U and ^{238}U concentrations for U(93.3) were extrapolated from those reported for the Godiva and Bigten assemblies and are detailed in Table 6.a. Additionally, the height was adjusted from the previous values of 119.392 cm and 44.239 cm to 121.0 cm and 44.4 cm, for Low-1 and Low-3 respectively, as indicated in references 13 and 20. Due to the relatively limited information, these benchmarks are recommended for inter-library comparisons only. The MCNP results are listed in Table 6.b.

Table 6.a: Specifications for Low Enrichment Uranium Cylinders

	Atomic Density [#/barn-cm]			
Nuclide	LA-12212 (10.9%)	LA-12212 (14.11%)	Low-1 (10.9%)	Low-3 (14.11%)
^{234}U	0.0	0.0	5.2859e-05	6.3454e-05
^{235}U	5.2027e-03	6.6555e-03	5.2028e-03	6.6552e-03
^{238}U	4.1992e-02	4.0001e-02	4.1940e-02	3.9939e-02

Table 6.b: MCNP Results for k_{eff} of the Low Enriched Uranium Cylinders

	ENDF/B-V	ENDF/B-VI
Low-1: 10.9%	1.0034 ± 0.0006	1.0002 ± 0.0005
Low-3: 14.11%	1.0017 ± 0.0006	0.9985 ± 0.0006

D. Graphite-tamped Uranium Sphere

The LA-12212 specifications for the graphite-tamped uranium sphere were referenced to LA-3067.[15] Given the specifications from LA-12212 (sphere of U(93.5% ^{235}U) with density 18.6 g/cc, and a 5.1 cm graphite reflector with ρ = 1.67 g/cc), no corresponding experiment was located in LA-3067. One possibility from LA-3067 is the sphere of nesting U(93.9) shells with an average ρ = 18.7 g/cc, surrounded by a 2" CS-312 graphite reflector with ρ = 1.67 g/cc, given in Table IC4a. However, due to a number of material and geometry inconsistencies between LA-3067 and LA-12212, this benchmark has been removed from our current suite.

E. Water-Reflected Uranium Sphere

The water-reflected uranium sphere geometry consists of a highly enriched uranium sphere, 97.67% ^{235}U or U(97.67), of radius 6.5537 cm immersed in a cylindrical tank of water which measured 30 cm in radius and 70 cm in height. For this benchmark, it is necessary to include the S(α, β) treatment for light water. No revisions were made to the water-reflected uranium sphere benchmark, and the specifications are well documented in the original publication. Table 7 gives the results for k_{eff} from the MCNP simulations and can be compared to the benchmark value of k_{eff} = 1.0003 ± 0.0005.

Table 7: MCNP Results for k_{eff} of the Water-Reflected Uranium Sphere

	ENDF/B-V	ENDF/B-VI
Water-Reflected Uranium Sphere	0.9948 ± 0.0008	0.9977 ± 0.0007

F. Three Uranium Cylinders

The three uranium cylinders benchmark was incorrectly referenced to an Oak Ridge National Laboratory report ORNL-2143[21] and should have been referenced to the report ORNL-2842[18], as indicated in Table 44 of LA-10860.[17] Some of the specifications were changed, or not included, in LA-10860, and we therefore standardized to the original specifications as given in ORNL-2842. ORNL-2842 describes this benchmark as three interacting 8-inch diameter aluminum cylinders of uranyl fluoride solution, $U(93.2)O_2F_2$, each having an aluminum wall thickness of 1/16 inch and a 0.015 inch edge-to-edge spacing in an equilateral triangle configuration. The solution concentration was as follows: 0.0812 g of U per g of solution, 0.0836 g of ^{235}U per cc of solution with a specific gravity of 1.105, and an atomic ratio of H: ^{235}U = 309. The cylinders were 16.3 inches in height with a total mass of ^{235}U of 3.39 kg for each. Due to uncertainties in the material specifications, this benchmark is recommended for inter-library comparisons only. The results of the MCNP simulations are given in Table 8.

Table 8: MCNP Results for k_{eff} of the Uranium Cylinders

	ENDF/B-V	ENDF/B-VI
Three Uranium Cylinders	0.9993 ± 0.0010	0.9953 ± 0.0010

G. 3x3 Array of Pu Fuel Rods

The last of the original nine benchmarks was for a 3x3 array of plutonium fuel rods each having 3 fuel cans separated by spacers, for an effective 3x3x3 array of fuel cans. Both the material specifications and geometry were modified from that described in LA-12212, based on the experimental description in reference 19. Figure 1 illustrates the experimental geometry, and the MCNP results are given in Table 9. Due to uncertainties in the material specifications, this benchmark is recommended for inter-library comparisons only.

Figure 1: Cross-Sectional View of 3x3 Array of Pu Fuel Rods[a]

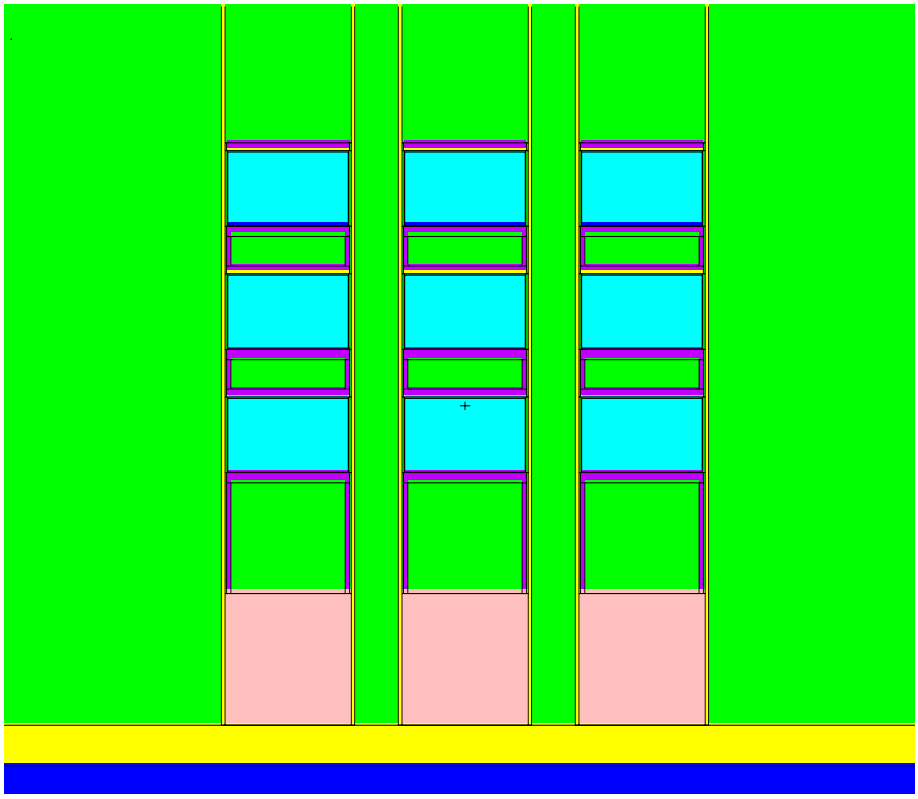

[a]The light blue areas contain the fuel and the bottom dark blue area shows the steel table support. All yellow areas are aluminum, the purple areas are aluminum spacers and heat sinks, the pink areas are mixtures of aluminum and iron, and the green areas are air.

Table 9: MCNP Results for k_{eff} of the 3x3 Array of Pu Fuel Rods

	ENDF/B-V	ENDF/B-VI
3x3 Array of Pu Fuel Rods	1.0081 ± 0.0007	1.0026 ± 0.0002

III. Additional Criticality Benchmarks

In addition to the two low-enriched uranium benchmarks mentioned previously, Low-2 and Low-4, another 35 benchmarks have been also implemented in the criticality problem suite. We have attempted to include a few benchmarks of each type (fast, thermal,

etc.) to give a broad range of information for the user. The test suite is still lacking representative benchmarks for lattices (the CSEWG specifications are incomplete), reactor problems at multiple temperatures, other reflected systems using various reflector materials, etc. We hope that these kinds of benchmarks can be added in the future. Table 10 lists the additional benchmarks and corresponding references.

Table 10: Additional Criticality Benchmarks

Benchmark Name	References
Low-2 (12.32%) and Low-4 (16.01%)	13, 15
ORNL-1 through ORNL-11	8, 23
PNL-1 through PNL-5, and PNL-11	8
Water-Reflected Pu Sphere	9
Pu Nitrate Solutions, Cases 2 and 4	9
Bigten, 1D and 2D	8, 22
Flattop-25	8
8” Nickel-reflected Oralloy Sphere	9
1.9” Tungsten-reflected Oralloy Sphere	9
6.5” Tungsten-reflected Oralloy Sphere	9
Flattop-Pu	8
U(N) reflected Pu Sphere	9
Thor (2 cases)	8, 9
Jezebel-23 (2 cases)	8, 9
Flattop-23	9
U(N) reflected U-233 (2 cases)	9

A. Low-Enriched Uranium

In LA-3067-MS, Rev. (1975), four experiments are documented (Table IA4) using repeated layers of highly enriched uranium, U(93.3), and natural uranium, U(N). The homogenized material for the four systems ranged from 10.9% to 16.01% ^{235}U by weight. Two of these systems, Low-1 (10.9%) and Low-3 (14.11%), have been described in the previous section. The remaining two, Low-2 (12.32%) and Low-4 (16.01%), have been implemented for completeness. As discussed previously, it is felt that this set of four benchmarks should be used primarily for inter-library comparisons. Table 11.a details the homogenized material specifications for the two new problems. The critical heights for Low-2 and Low-4 were 60.8 ± 0.3 cm and 34.7 ± 0.3 cm respectively. The results from the MCNP calculations are listed in Table 11.b.

Table 11.a: Specifications for Low Enrichment Uranium Cylinders (12.32%) and (16.01%)

	Atomic Density [#/barn-cm]	
Nuclide	Low-2 (12.32%)	Low-4 (16.01%)
^{234}U	5.5731e-05	7.3398e-05
^{235}U	5.8187e-03	7.5818e-03
^{238}U	4.1355e-02	3.9698e-02

Table 11.b: MCNP Results for k_{eff} of the Low Enrichment Uranium Cylinders (12.32%) and (16.01%)

	ENDF/B-V	ENDF/B-VI
Low-2: 12.32%	1.0029 ± 0.0007	1.0023 ± 0.0005
Low-4: 16.01%	1.0050 ± 0.0006	1.0007 ± 0.0006

B. Thermal Systems for ^{235}U and ^{239}Pu

1. Unreflected Spheres of Uranyl Nitrate Solutions

The ORNL series of five CSEWG benchmarks, T1-T5, are unreflected spheres of uranyl nitrate in water containing various concentrations of ^{10}B. The T1-T5 benchmarks are designated as ORNL-1 through ORNL-4, and ORNL-10 respectively. ORNL-1 and ORNL-10 have no ^{10}B present. ORNL-1 through ORNL-4 each have a radius of 34.595 cm, while ORNL-10 has a radius of 61.011 cm. The results from MCNP calculations are listed in Table 12. The measured eigenvalues were corrected for various sources of room return, departures from sphericity, and delayed-neutron importance.

Table 12: MCNP Results for k_{eff} of the ORNL Series of Benchmarks

	Corrected Measured	ENDF/B-V	ENDF/B-VI
ORNL-1 (T1)	1.00026	1.0001 ± 0.0006	0.9965 ± 0.0006
ORNL-2 (T2)	0.99975	0.9985 ± 0.0006	0.9955 ± 0.0006
ORNL-3 (T3)	0.99994	0.9970 ± 0.0006	0.9931 ± 0.0007
ORNL-4 (T4)	0.99924	0.9991 ± 0.0007	0.9947 ± 0.0006
ORNL-10 (T5)	1.00031	1.0003 ± 0.0004	0.9967 ± 0.0004

2. Unreflected Spheres of Plutonium Nitrate Solutions

The PNL series of CSEWG benchmarks, T13-T17, corresponding to PNL-1 through PNL-5, is based on a set of unreflected spheres of plutonium nitrate solutions. These benchmarks are useful for testing both fast scattering and thermal absorption from the water, and the thermal capture and fission cross sections for ^{239}Pu. PNL-1 and PNL-2 have an effective radius of 19.509 cm with H: ^{239}Pu ratios of 700 and 131 respectively, and contain 4.6% (by weight) ^{240}Pu. PNL-3 and PNL-4 have an effective radius of 22.70 cm and 4.20 wt. % of ^{240}Pu, with H: ^{239}Pu ratios of 1204 and 911 respectively. PNL-5 has an effective radius of 20.1265 cm, H: ^{239}Pu ratio of 578, and contains 4.17 wt. % ^{240}Pu. The specifications were derived for a corrected k_{eff} value equal to 1.0.

There are additional CSEWG benchmarks for the PNL series of plutonium spheres and cylinders, T24-T30 corresponding to PNL-6 through PNL-12. These additional benchmarks contain relatively small amounts of ^{241}Pu and ^{242}Pu. However, PNL-10 and PNL-11 are cylindrical models which have higher concentrations of ^{240,241,242}Pu, and PNL-11 has the highest concentration of these isotopes with 42.86 atom weight % of ^{240}Pu, 10.75 at. % ^{241}Pu, and 4.66 at. % ^{242}Pu. The PNL-11 (CSEWG: T29) benchmark has been included in this set. The MCNP results for the PNL benchmarks are given in Table 13.

Table 13: MCNP Results for k_{eff} of the PNL Series of Benchmarks

	ENDF/B-V	ENDF/B-VI
PNL-1 (T13)	1.0173 ± 0.0009	1.0063 ± 0.0009
PNL-2 (T14)	1.0075± 0.0010	1.0003 ± 0.0011
PNL-3 (T15)	0.9978 ± 0.0008	0.9899 ± 0.0008
PNL-4 (T16)	1.0045 ± 0.0009	0.9951 ± 0.0009
PNL-5 (T17)	1.0089 ± 0.0009	0.9996 ± 0.0009
PNL-11 (T29)	1.0076 ± 0.0008	1.0012 ± 0.0007

3. Water-Reflected Plutonium Sphere, ICSBEP: PU-MET-FAST-011

The ICSBEP benchmark PU-MET-FAST-011 is a sphere of alpha-phase plutonium surrounded by a spherical shell of water. The outer radii for the plutonium core and water reflector are 4.1217 cm and 29.5217 cm respectively. This benchmark is listed with the other thermal benchmarks as it also requires the use of $S(\alpha, \beta)$ data for light water. The experimental k_{eff} value was 0.98, with a corrected experimental k_{eff} of 1.000 ± 0.001. The MCNP results are given in Table 14.

Table 14: MCNP Results for k_{eff} of the Water-Reflected Plutonium Sphere

	ENDF/B-V	ENDF/B-VI
Water-Reflected Plutonium Sphere	1.0083 ± 0.0009	0.9990 ± 0.0010

4. Plutonium Nitrate Solutions, ICSBEP: PU-SOL-THERM-003

The ICSBEP benchmark PU-SOL-THERM-003 is composed of a series of water-reflected 13” diameter spheres of plutonium nitrate solutions. The plutonium nitrate solutions were contained by a thin shell of stainless steel or aluminum. This report includes cases 2 and 4 from this series both of which use a stainless steel container. Case 2 has 1.76% (by weight) ^{240}Pu and 34.32g of Pu/L of solution, while Case 4 has 3.12% (by weight) ^{240}Pu and 38.12g of Pu/L of solution. The outer radii for the plutonium nitrate solution, stainless steel container and water reflector were the same for both cases, with values of 16.5156, 16.6426, and 46.6426 cm respectively. The corrected experimental values for k_{eff} were 1.000, and the uncertainties were estimated to be ± 0.0035. The MCNP results are given in Table 15.

Table 15: MCNP Results for k_{eff} of PU-SOL-THERM-003

	ENDF/B-V	ENDF/B-VI
Case 2	1.0092 ± 0.0008	1.0013 ± 0.0005
Case 4	1.0120 ± 0.0008	1.0034 ± 0.0008

C. Other Reflected Systems

The MCNP results for the remaining reflected systems described below are given in Table 16.

1. Bigten 1D and 2D, CSEWG: F20

The CSEWG benchmark Bigten, F20, has both a one- and two-dimensional model description for the U(10) core reflected by depleted-uranium metal. The one-dimensional spherical model has an outer core radius of 30.48 cm and an outer reflector radius of 45.72 cm. The two-dimensional model is a cylindrical core, having a radius of 26.67 cm and a total length of 55.88 cm, centered in a cylindrical reflector with an outer radius of 41.91 cm and a total length of 96.52 cm.

2. Flattop-25, CSEWG: F22

Flattop-25 (CSEWG: F22) is a U(N) reflected sphere of highly enriched uranium, and emphasizes the fission-source energy range in ^{238}U. The spherical model has a core radius of 6.116 cm surrounded by a natural uranium spherical shell with an outer radius of 24.13 cm.

3. ICSBEP: HEU-MET-FAST-003

The ICSBEP benchmark HEU-MET-FAST-003 is a set of 12 reflected oralloy spheres. For this report, we have chosen to include three of the 12 models; the 8” nickel reflector, 1.9” tungsten carbide reflector, and the 6.5” tungsten carbide reflector. The nickel reflected model has an oralloy core radius of 6.4627 cm and an outer nickel radius of 26.7827 cm. The 1.9” and 6” tungsten-carbide reflected models have outer core radii of 6.6020 cm and 6.0159 cm, with outer reflector radii of 11.4280 cm and 22.5259 cm respectively.

4. Flattop-Pu, CSEWG: F23

Flattop-Pu is a spherical Pu metal core (4.5% ^{240}Pu) surrounded by a natural uranium reflector, U(N). The core and reflector have radii of 4.533 cm and 24.13 cm respectively.

5. ICSBEP: Pu-MET-FAST-010

The ICSBEP benchmark PU-MET-FAST-010 is a delta-phase plutonium sphere surrounded by a spherical U(N) reflector, having outer radii of 5.0419 cm and 9.1694 cm respectively.

6. Thor, CSEWG: F25 and ICSBEP: PU-MET-FAST-008

The one-dimensional Thor benchmark is a spherical delta-phase Pu core (5.1% ^{240}Pu) surrounded by a natural thorium reflector. This benchmark is described by both CSEWG and ICSBEP. CSEWG: F25 specifies the core and reflector to have outer radii of 5.310 cm and 29.88 cm respectively, with a benchmark k_{eff} value of 1.000 ± 0.001. The one-dimensional model from the ICSBEP benchmark PU-MET-FAST-008 specifies the

same core and reflector geometry, with a benchmark k_{eff} value of 1.000 ± 0.0006. The two-dimensional model for PU-MET-FAST-008 specifies a spherical Pu metal core of radius 5.310 cm, surrounded by a cylindrical natural thorium reflector having a height of 53.34 cm and an outer radius of 26.68 cm. The material specifications for both PU-MET-FAST-008 models are the same. The results of the CSEWG and two-dimensional PU-MET-FAST-008 model are given in Table 16.

Table 16: MCNP Results for k_{eff} for Other Reflected Systems

	Benchmark	ENDF/B-V	ENDF/B-VI
Bigten-1D, CSEWG: F20	0.996 ± 0.003	1.0035 ± 0.0007	1.0060 ± 0.0007
Bigten-2D, CSEWG: F20	0.996 ± 0.002	1.0026 ± 0.0007	1.0054 ± 0.0008
Flattop-25, CSEWG: F22	1.000 ± 0.001	1.0045 ± 0.0010	1.0041 ± 0.0009
HEU-MET-FAST-003: 8” nickel	1.000 ± 0.005	1.0143 ± 0.0008	1.0048 ± 0.0007
HEU-MET-FAST-003: 1.9” tungsten carbide	1.000 ± 0.005	0.9986 ± 0.0008	1.0062 ± 0.0008
HEU-MET-FAST-003: 6.5” tungsten carbide	1.000 ± 0.005	1.0036 ± 0.0007	1.0099 ± 0.0008
Flattop-Pu, CSEWG: F23	1.000 ± 0.001	1.0069 ± 0.0010	1.0036 ± 0.0010
PU-MET-FAST-010	1.0000 ± 0.0018	1.0063 ± 0.0010	0.9999 ± 0.0009
Thor, CSEWG: F25	1.000 ± 0.001	1.0150 ± 0.0009	1.0073 ± 0.0009
Thor, PU-MET-FAST-008	1.000 ± 0.006	1.0149 ± 0.0010	1.0093 ± 0.0008

E. ^{233}U systems

The MCNP results for the ^{233}U systems described below are given in Table 17.

1. Jezebel-23; CSEWG: F19 and ICSBEP: U233-MET-FAST-001

Jezebel-23 is a bare metal sphere of ^{233}U. Both CSEWG and ICSBEP specifications give a benchmark k_{eff} of 1.000 ± 0.001, with slightly different material and core radius specifications (see Table 18).

2. Flattop-23; CSEWG: F24

Flattop-23 (CSEWG: F24) is a U(N) reflected core of ^{233}U metal. CSEWG: F24 has a small 0.293 cm gap between the core and U(N) reflector. The outer radii for the core, gap, and reflector are 4.317, 4.610, and 24.13 cm respectively.

3. ICSBEP: U233-MET-FAST-003

There are two similar models to Flattop-23 from ICSBEP: U233-MET-FAST-003, 10 kg and 7.6 kg. The 10 kg model has a ^{233}U metal core radius of 5.0444 cm, surrounded by a

U(N) reflector with an outer radius of 7.3456. The 7.6 kg model has a core radius of 4.5999 cm and an outer U(N) reflector radius of 9.9085 cm. For both models, the gap between the core and reflector has been adjusted for in the specifications. The specified value of k_{eff} for both U233-MET-FAST-003 models is 1.000 ± 0.001.

4. ORNL-5 through ORNL-9, ORNL-11

The series of benchmarks designated as ORNL-5 through ORNL-9 and ORNL-11 are unreflected spheres of uranyl nitrate in water with ^{233}U as the fuel.[23] ORNL-5 through ORNL-9 have radii of 34.595 cm, whereas ORNL-11 has a radius of 61.011 cm. ORNL-5 and ORNL-11 have no ^{10}B; ORNL-6 through ORNL-9 contain various concentrations of ^{10}B. These benchmarks are useful for testing both fast scattering and thermal absorption from the water, as well as the thermal absorption of ^{235}U and ^{233}U. Table 17 lists the corrected experimental values and MCNP results for each of the ORNL benchmarks. The experimental values were corrected for new β values, the thin Al container vessels, distortion of the spherical shape, etc. No error bars were given for the corrected measured values.

Table 17: MCNP Results for k_{eff} for ^{233}U Systems

	Benchmark	ENDF/B-V	ENDF/B-VI
Jezebel-23, CSEWG: F19	1.000 ± 0.001	0.9922 ± 0.0008	0.9921 ± 0.0008
Jezebel-23, U233-MET-FAST-001	1.000 ± 0.001	0.9937 ± 0.0004	0.9935 ± 0.0004
Flattop-23, CSEWG: F24	1.000 ± 0.001	1.0020 ± 0.0011	1.0036 ± 0.0010
U233-MET-FAST-003: 7.6 kg	1.000 ± 0.001	1.0002 ± 0.0010	0.9998 ± 0.0009
U233-MET-FAST-003: 10 kg	1.000 ± 0.001	0.9964 ± 0.0009	0.9982 ± 0.0009
ORNL-5[23]	0.99949	0.9987 ± 0.0006	0.9949 ± 0.0006
ORNL-6[23]	1.00009	0.9984 ± 0.0005	0.9965 ± 0.0005
ORNL-7[23]	1.00015	0.9993 ± 0.0007	0.9972 ± 0.0006
ORNL-8[23]	0.99930	0.9992 ± 0.0006	0.9966 ± 0.0005
ORNL-9[23]	0.99942	0.9969 ± 0.0006	0.9944 ± 0.0006
ORNL-11[23]	0.99944	0.9975 ± 0.0004	0.9956 ± 0.0004

Table 18: Specifications for Jezebel-23

Nuclide	Atomic Density [#/barn-cm]	
	CSEWG: F19 (R = 5.983 cm)	U233-MET-FAST-001 (R = 5.9838 cm)
^{233}U	4.671e-02	4.6712e-02
^{234}U	5.900e-04	5.9026e-04
^{235}U	1.000e-05	1.4281e-05
^{238}U	2.900e-04	2.8561e-04

IV. Discussion of Other Experimental Data Available for Criticality Benchmarks

In addition to the standard k_{eff} measurement, other experimental measurements were performed for a variety of critical assemblies such as Godiva and Jezebel. The experimental measurements included the central fission and activation ratios for a variety of nuclides, and measurements of the neutron leakage spectra. These measurements can sometimes provide more detailed information on the accuracy of the nuclear data used in the calculations than can the integral k_{eff} measurement. Our primary source for this additional experimental information is the CSEWG benchmark specifications, and the implementation of these measurements for Godiva based on the CSEWG: F5 specifications is discussed in detail below.

A. Central Fission and Activation Ratios

Two types of experimental measurements for Godiva were the central fission and central activation ratios. The central fission ratio is the ratio of $\sigma_{n,fission}$ for a particular isotope to the value of $\sigma_{n,fission}$ for ^{235}U, measured near the center of the Godiva assembly. The central activation ratio is the ratio of $\sigma_{n,\gamma}$ for a particular isotope to $\sigma_{n,fission}$ for ^{235}U, again measured near the center of Godiva. Four central fission ratio measurements and five central activation ratio measurements were performed for Godiva and are described in the CSEWG benchmark specifications.

1. Description of Calculational Methods

These measurements may be calculated using several methods. First, an FM multiplier card can be used to multiply an F4 (neutron flux) tally calculated over the volume of an imaginary sphere of radius R_o (smaller than Godiva itself) placed at the center of the Godiva assembly. The FM multiplier card was used to weight the F4 tally by $\sigma_{n,fission}$ for ^{235}U, and to weight the F4 tally by either $\sigma_{n,fission}$ or $\sigma_{n,\gamma}$ for each nuclide of interest. The weighted tally result for each nuclide is then divided by the $\sigma_{n,fission}$ ^{235}U result to

obtain the ratio of interest. For example, to calculate the central fission ratio for ^{237}Np, the F4 tally was multiplied by $\sigma_{n,fission}$ for ^{237}Np, and then divided by the $\sigma_{n,fission}$ weighted F4 tally for ^{235}U. It was determined that the F4 tally ratios were insensitive to the choice of R_o. This method will be referred to as the "FM4 method."

Secondly, an FM multiplier card can be used to multiply a point detector (F5) tally calculated at the center of Godiva. This method is like the FM4 method, except that a point detector tally is used in place of the F4 tally. For example, the central activation ratio for ^{55}Mn was calculated by multiplying the F5 tally by $\sigma_{n,\gamma}$ for ^{55}Mn, then dividing by the $\sigma_{n,fission}$ weighted F5 tally for ^{235}U. It was determined that the F5 tally ratios were insensitive to the choice of R_e for values of R_e less than 0.5 mean free paths (about 1.35 cm for Godiva). This method will be referred to as the "FM5 method."

Finally, the actual experimental procedure used to measure the ratios can be modeled (see the paper by Byers[11]). This procedure is like the FM4 method, except that the F4 tally is taken over the volume of a thin disk in the center of Godiva. Just as with the first two methods, the F4 tally is then multiplied by $\sigma_{n,fission}$ or $\sigma_{n,\gamma}$ for each nuclide, and the ratio to the $\sigma_{n,fission}$ weighted ^{235}U tally is taken. The disk represents the thin foils that were inserted into Godiva to measure the activation ratios. The actual material was not placed in the disk volume since calculations showed that the presence of the material did not significantly perturb the neutron flux. Instead, the disk was filled with the same material as the rest of Godiva. This technique allowed the ratios for all nuclides of interest to be calculated in one run. Since the volume of the disk was so small, runs took about 13 hours to yield results with acceptable uncertainties. This method will be referred to as the "thin foil method."

2. Comparison of Results

The results from all three methods were statistically equivalent. To compare the results from any two methods, ratios of the results from each method were taken. First, the ratio of the FM4 result to the FM5 result was taken for each nuclide. The uncertainty in each ratio was determined by propagating the uncertainties in the FM4 and FM5 results. For each of the nine nuclides, the ratio of the FM4 to FM5 result was within one standard deviation of 1.0. For the FM4 method, R_o was taken to be 1 cm. For the FM5 method, R_e was taken to be 1.35 cm or about 0.5 mean free paths. Second, ratios of the FM4 results to the thin foil results were taken. Again, the ratio of the FM4 result to the thin foil result for each of the nine nuclides was within one standard deviation of 1.0.

3. Discussion of the Thin Foil Results

Since all three methods gave statistically equivalent results, only the thin foil method results will be presented. The central fission ratios for each isotope are listed in Table 19, and the central activation ratios are listed in Table 20. As the ENDF/B-V based data libraries only contain data for natural Cu, the central activation ratio for ^{63}Cu cannot be calculated for ENDF/B-V. All results were calculated using 3000 kcode cycles and 10,000 histories per cycle.

It is important to note that the Godiva benchmark is represented as a perfect sphere of homogeneous material, whereas the actual assembly was neither perfectly spherical nor homogeneous. Additionally, the response of the detectors used to measure the neutron fluxes in the Godiva experiments was not modeled, nor was the neutron return from the room or supporting assemblies. Despite the idealizations of the benchmark calculations, the agreement between MCNP and experiment is good for most isotopes. Some conclusions based on these results will be discussed in Section V.

Table 19: Central Fission Ratios

Nuclide	CSEWG	MCNP ENDF/B-V	B-V to CSEWG Ratio	MCNP ENDF/B-VI	B-VI to CSEWG Ratio
^{233}U	1.59 ± 0.03	1.5685 ± 0.0104	0.987 ± 0.020	1.5917 ± 0.0110	1.001 ± 0.020
^{238}U	0.1647 ± 0.0018	0.1708 ± 0.0015	1.037 ± 0.015	0.1613 ± 0.0017	0.979 ± 0.015
^{237}Np	0.837 ± 0.013	0.8941 ± 0.0066	1.062 ± 0.018	0.8267 ± 0.0068	0.988 ± 0.017
^{239}Pu	1.402 ± 0.025	1.3964 ± 0.0094	0.996 ± 0.019	1.3864 ± 0.0098	0.989 ± 0.019

Table 20: Central Activation Ratios

Nuclide	CSEWG	MCNP ENDF/B-V	B-V to CSEWG Ratio	MCNP ENDF/B-VI	B-VI to CSEWG Ratio
^{55}Mn	0.0027 ± 0.0002	0.00300 ± 0.00004	1.109 ± 0.084	0.00339 ± 0.00004	1.256 ± 0.094
^{59}Co	0.038 ± 0.003	0.00598 ± 0.00011	0.157 ± 0.013	0.00575 ± 0.00029	0.151 ± 0.014
^{63}Cu	0.0117 ± 0.0006	---	---	0.01145 ± 0.00010	0.979 ± 0.051
^{93}Nb	0.030 ± 0.003	0.02938 ± 0.00022	0.979 ± 0.098	0.03389 ± 0.00024	1.130 ± 0.113
^{197}Au	0.100 ± 0.002	0.08577 ± 0.00083	0.858 ± 0.019	0.09313 ± 0.00065	0.931 ± 0.020

B. Neutron Leakage and Flux Spectra

The final quantities calculated for Godiva were the neutron leakage spectrum and the average internal neutron flux. The neutron leakage spectrum is the average current of neutrons across Godiva's outer surface and has been measured experimentally. The paper by Stewart[12] gives the experimental leakage spectrum evaluated in 29 energy bins. In the CSEWG summary,[23] the leakage spectrum is further condensed to 8 energy bins. The F1 leakage tally from MCNP was binned according to both of these schemes and compared. Figure 2 compares the results from ENDF/B-V and ENDF/B-VI to the leakage given in CSEWG. Figure 3 compares the results from ENDF/B-V and ENDF/B-VI to the leakage given in Stewart's paper. Each leakage spectrum was normalized to an area of 1 for easy comparison.

From the neutron leakage plots it is clear that the experimental leakage at low energy is consistently higher than the calculated leakage. One contributing factor is the background sources of low-energy neutrons in the actual experiments. As mentioned previously, this was not modeled in the MCNP runs. Above ~ 6 MeV, the apparent discrepancies between Figures 2 and 3 are due to the energy bins chosen.

Figures 2 and 3 qualitatively show that ENDF/B-VI agrees better with experiment than ENDF/B-V, especially at low energy. As a more quantitative comparison, the chi-squared difference between MCNP and the experimental data was calculated for each bin structure. The χ^2 difference between any two histograms can be defined as:

$$\chi^2 = \sum_i \frac{(MCNP(i) - Data(i))^2}{MCNP(i) + Data(i)}$$

where Data(i) is the experimental leakage in bin i, MCNP(i) is the MCNP-calculated leakage in bin i, and the sum is over the number of energy bins.[24] The values of χ^2 for each pair of histograms are listed in matrix form in Table 21. Notice that the ENDF/B-VI spectra agree much better with the experimental spectra; the values of χ^2 for ENDF/B-VI are less than 1/2 the corresponding values for ENDF/B-V.

Table 21: χ^2 Difference Between MCNP and Experimental Leakage Plots

	χ^2 Difference Relative to CSEWG Spectrum	χ^2 Difference Relative to Stewart Spectrum
MCNP/B-V	0.0307	0.0562
MCNP/B-VI	0.0046	0.0222

The average internal neutron flux is the average flux of neutrons throughout Godiva and is calculated with an F4 tally. Although no experimental measure of this quantity exists, we have included comparisons of the F4 tally results from ENDF/B-V and ENDF/B-VI in Figures 4 and 5. Figure 4 uses a linear energy scale to clarify the high-energy end of the spectrum, while Figure 5 uses a logarithmic scale to show the lower energy region more clearly.

V. Summary and Recommendations for a Test Suite of Criticality Benchmarks

The original set of nine criticality benchmarks from LA-12212 has been reviewed, with seven of the benchmarks revised, one removed from the set, and the remaining benchmark implemented as described in the original report. In addition, many criticality

benchmarks have been added to the test suite. Currently, the test suite contains high-quality benchmark descriptions for 35 assemblies, and descriptions of six benchmarks that are recommended for inter-library comparisons only. There are multiple benchmark specifications for the Godiva, Jezebel-4.5%, Jezebel-20.1%, Jezebel-23, Thor, and Bigten assemblies depending on the reference source and the geometry (1D or 2D) that is used. Table 22 describes the criticality benchmarks in the current test suite.

The ENDF/B-V and ENDF/B-VI results from these benchmarks indicate that the new evaluation for ^{239}Pu is greatly improved. The B-VI evaluation for ^{235}U is improved for fast systems, but it does not perform as well as B-V for thermal systems such as the ORNL spheres. The ORNL spheres of uranyl nitrate in water with ^{235}U as fuel give an average Δk_{eff} = -0.0037 for ENDF/B-VI relative to B-V. This value is larger than the average difference of Δk_{eff} = -0.0025 seen for the ORNL spheres with ^{233}U as fuel. As the evaluation for ^{233}U did not change from ENDF/B-V to B-VI, it can be concluded this difference is due largely to the new evaluations for ^{1}H, ^{10}B, ^{16}O, and ^{14}N, which make up the majority of the material for these assemblies. For the U233-MET-FAST-003 benchmark, the contributions from ^{234}U, ^{235}U and ^{238}U increased k_{eff} from ENDF/B-V to ENDF/B-VI by 0.0018 for the 10 Kg model and decreased k_{eff} by 0.0004 for the 7.6 Kg model.

The expansion of the Godiva benchmark to include other experimental measurements that were performed gave interesting results. For all the nuclides used in the central fission and activation ratio measurements, new evaluations were performed for ENDF/B-VI. The central fission ratio measurements indicated an improvement in the ENDF/B-VI evaluation for ^{237}Np, and gave approximately equivalent results for ^{233}U and ^{239}Pu. While the results for ^{238}U changed dramatically, there is still room for improvement. The central activation ratio measurements indicated an improvement for ^{197}Au, and good agreement for ^{63}Cu. The results for ^{55}Mn and ^{93}Nb are worse for ENDF/B-VI, whereas the results for ENDF/B-V and B-VI are both very poor for ^{59}Co. There is still room for improvement for ^{197}Au. A comparison of the measured leakage spectrum for the Godiva assembly showed improvement from ENDF/B-V to ENDF/B-VI, though the flux is still underestimated in the lowest energy regions and overestimated at higher energies. A contributing factor to the leakage spectra differences is believed to be the simplification of the benchmark specifications relative to the actual experimental geometry.

Although the suite of criticality benchmarks has been greatly expanded, a need still exists for other types of criticality benchmarks such as lattices, reactor problems at multiple temperatures, and other reflected systems using various reflector materials. Additionally, we plan to further expand the CSEWG-based benchmarks for Jezebel-(4.5%), Jezebel-(20.1%), Jezebel-23, Bigten, Flattop-25, Flattop-Pu, Flattop-23, and Thor. We also plan to perform sensitivity studies to determine the major contributor to the difference in k_{eff} for assemblies impacted by cross sections for the light elements.

Table 22: Summary of Benchmarks

Experiment Name / Model Used	Description
Uranium-Fueled Assemblies: Unreflected	
Godiva CSEWG: F5 ICSBEP: Simple Sphere ICSBEP: Nested Spherical Shells	Sphere of highly enriched uranium
Jezebel-23 CSEWG: F19 ICSBEP: U233-MET-FAST-001	Bare metal sphere of ^{233}U
ORNL-1	Unreflected spheres of uranyl nitrate in water with various concentrations of ^{10}B and using ^{235}U as fuel
ORNL-2	
ORNL-3	
ORNL-4	
ORNL-10	
ORNL-5	Unreflected spheres of uranyl nitrate in water with various concentrations of ^{10}B and using ^{233}U as fuel
ORNL-6	
ORNL-7	
ORNL-8	
ORNL-9	
ORNL-11	
Uranium-Fueled Assemblies: Reflected	
Water-Reflected Uranium Sphere	HEU sphere in cylindrical tank of water
Bigten 1D Model -- CSEWG: F20 2D Model -- CSEWG: F20	Cylindrical core of uranium (10% ^{235}U) reflected by depleted-uranium metal
Flattop-25 / CSEWG: F22	HEU sphere reflected by shell of natural uranium
ICSBEP: HEU-MET-FAST-003 (8'' nickel)	Oralloy sphere reflected by 8'' of nickel
ICSBEP: HEU-MET-FAST-003 (1.9'' tungsten)	Oralloy sphere reflected by 1.9'' tungsten carbide
ICSBEP: HEU-MET-FAST-003 (6.5'' tungsten)	Oralloy sphere reflected by 6.5'' tungsten carbide
Flattop-23 / CSEWG: F24	Sphere of ^{233}U reflected by natural uranium
ICSBEP: U233-MET-FAST-003 7.6 kg Model 10.0 kg Model	Sphere of ^{233}U reflected by natural uranium
Plutonium-Fueled Assemblies: Unreflected	
Jezebel (4.5%) CSEWG: F1 ICSBEP: PU-MET-FAST-001	Sphere of nickel-clad plutonium metal with 4.5 wt. % ^{240}Pu

Table 22 continued

Experiment Name / Model Used	Description
Jezebel (20.1%) CSEWG: F21 ICSBEP: PU-MET-FAST-002	Sphere of nickel-clad plutonium metal with 20.1 wt. % ^{240}Pu
PNL-1	Unreflected spheres of plutonium nitrate solutions with different wt. % of ^{240}Pu
PNL-2	
PNL-3	
PNL-4	
PNL-5	
PNL-11	
Plutonium-Fueled Assemblies: Reflected	
Flattop-Pu / CSEWG: F23	Spherical plutonium core reflected by shell of natural uranium
ICSBEP: PU-MET-FAST-010	Sphere of delta-phase plutonium reflected by sphere of natural uranium
Water-Reflected Plutonium Sphere / ICSBEP: PU-MET-FAST-011	Sphere of alpha-phase plutonium surrounded by spherical shell of water
Plutonium Nitrate Solution (case 2) / ICSBEP: PU-SOL-THERM-003	Sphere of water-reflected plutonium nitrate solution -- 1.76 wt. % ^{240}Pu
Plutonium Nitrate Solution (case 4) / ICSBEP: PU-SOL-THERM-003	Sphere of water-reflected plutonium nitrate solution -- 3.12 wt. % ^{240}Pu
Thor CSEWG: F25 ICSBEP: PU-MET-FAST-008	Sphere of delta-phase plutonium reflected by natural thorium
Assemblies for Inter-library Comparisons Only:	
Low-1	Cylinders of layered plates of enriched ^{235}U and natural uranium
Low-2	
Low-3	
Low-4	
Three Uranium Cylinders	Three aluminum cylinders containing uranyl fluoride solution positioned in an equilateral triangle
3x3 Array of Pu Fuel Rods	3x3x3 array of Pu fuel cans

Figure 2:
ENDF/B-V and ENDF/B-VI vs. CSEWG Leakage for Godiva

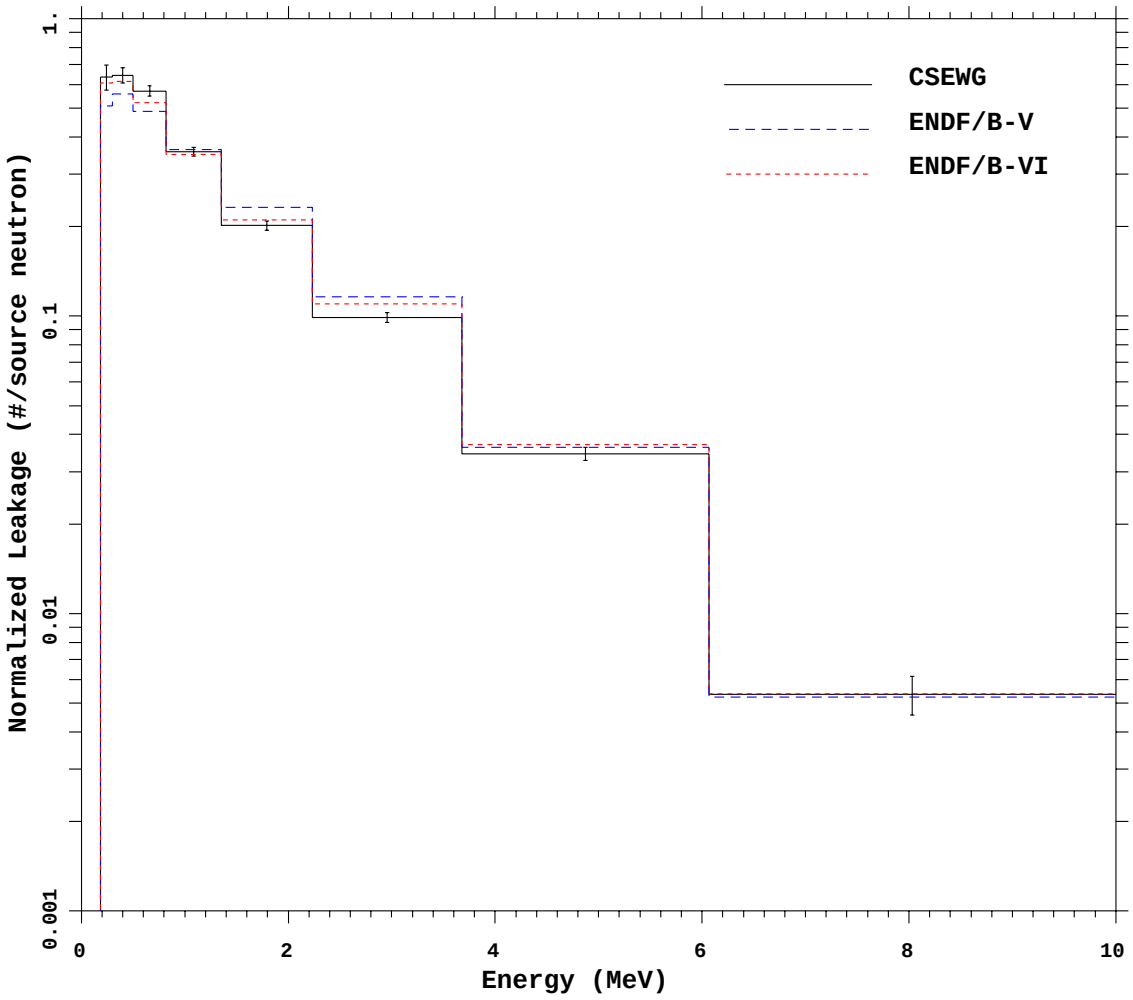

Figure 3:
ENDF/B-V and ENDF/B-VI vs. Experimental (Stewart) Leakage for Godiva

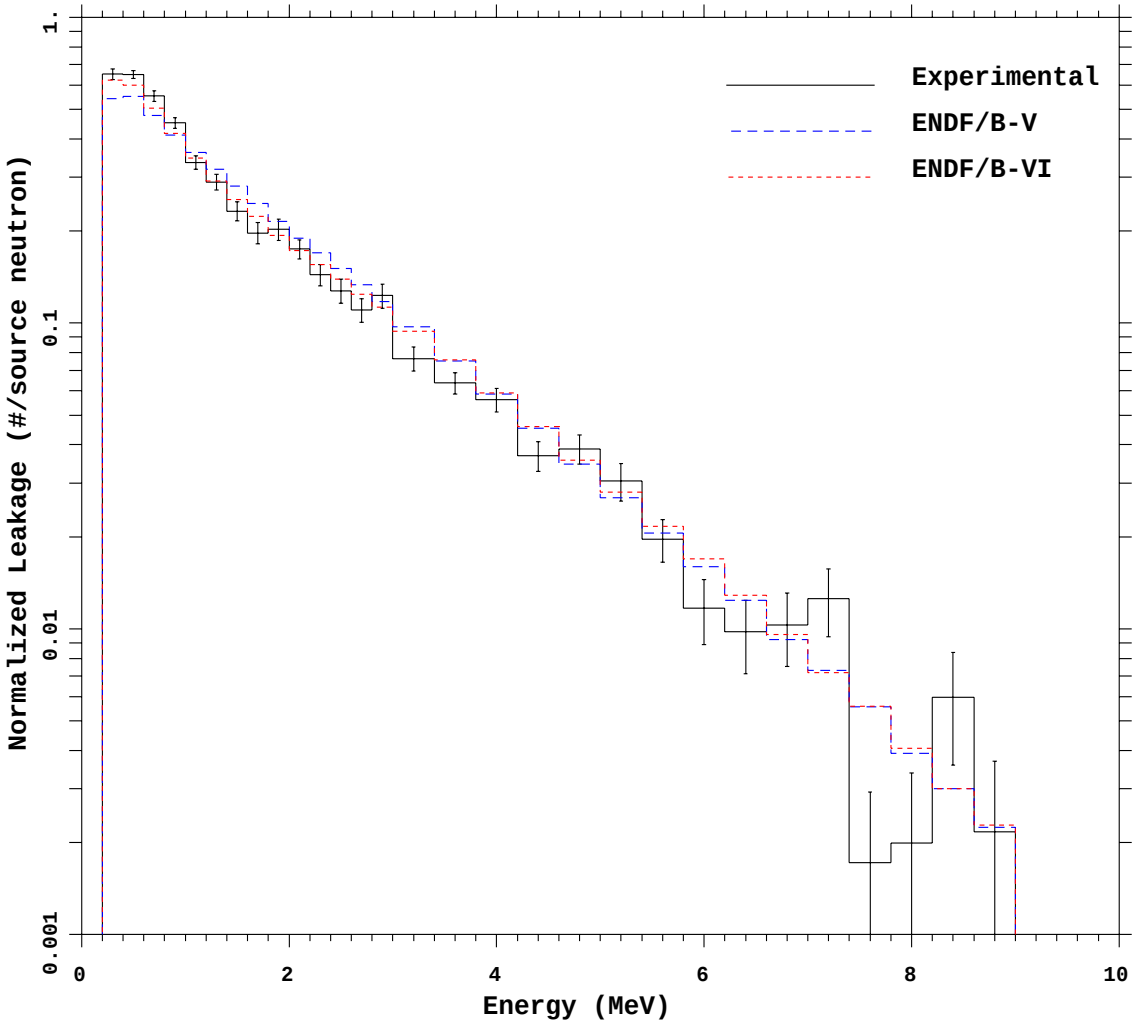

Figure 4:
ENDF/B-V vs. ENDF/B-VI Neutron Flux (F4) Tally for Godiva

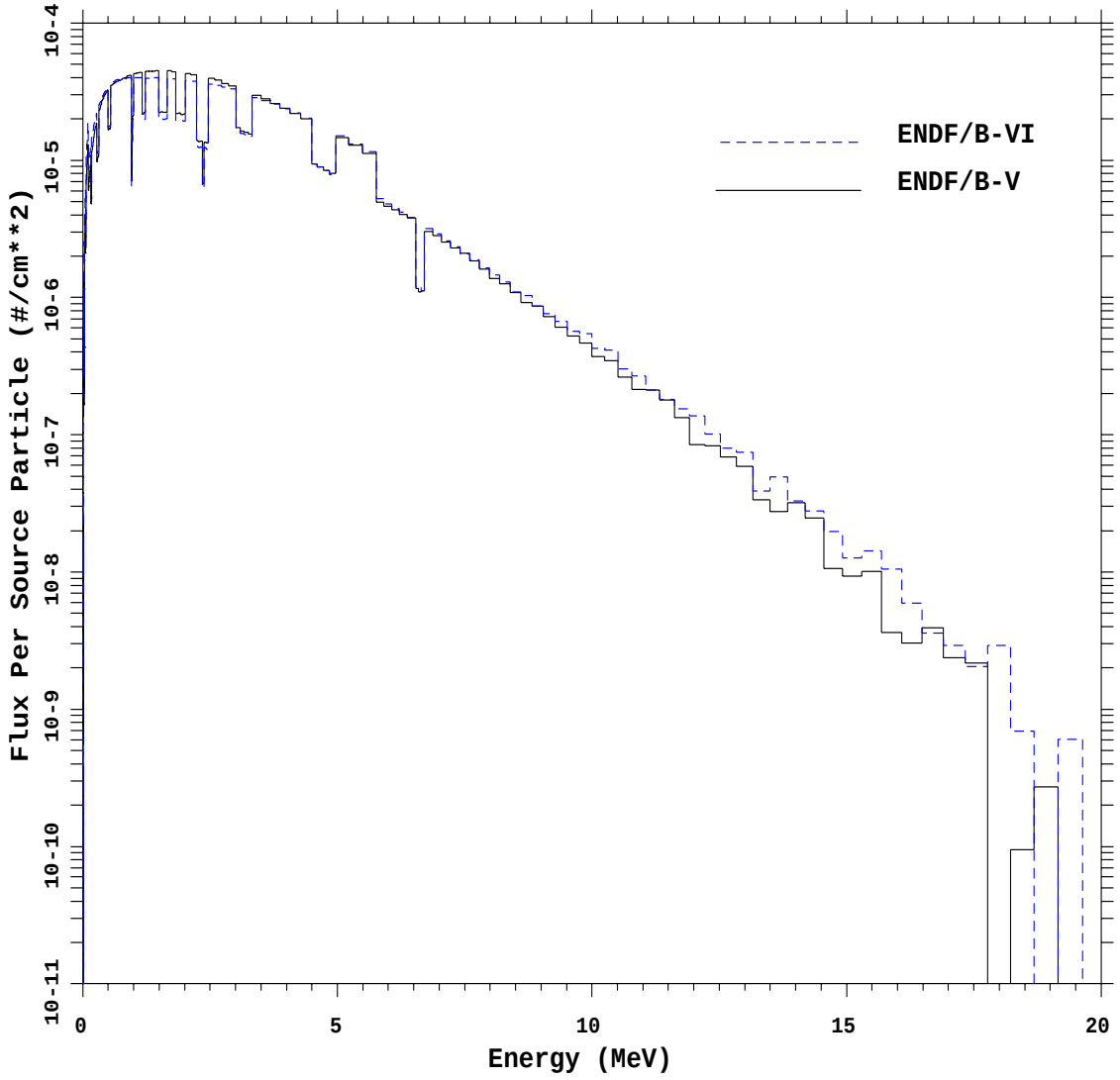

Figure 5:
ENDF/B-V vs. ENDF/B-VI Neutron Flux (F4) Tally for Godiva

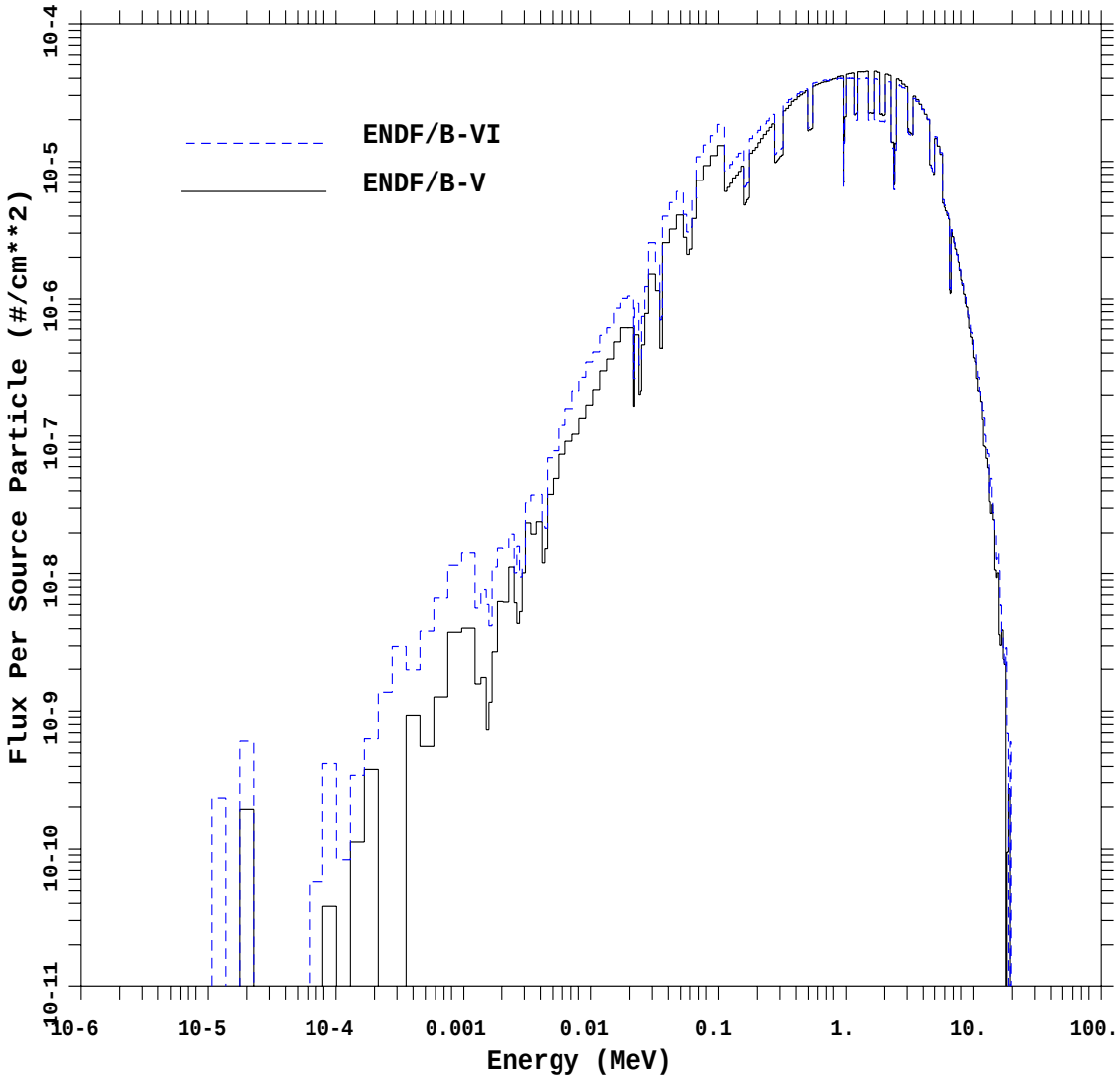

VIII. Acknowledgments

We wish to acknowledge the following for useful discussions and help in acquiring the references: Roger Brewer, Pete Jaegers, Bob MacFarlane, Russ Mosteller, and Laurie Waters.

IX. References

1 J. F. Briesmeister, Ed., “MCNP4A - A General Monte Carlo N-Particle Transport Code,” Los Alamos National Laboratory report, LA-12625-M (1993).

2 J. S. Hendricks, S. C. Frankle, and J. D. Court, “ENDF/B-VI Data for MCNP,” Los Alamos National Laboratory report and errata, LA-12891 (1994).

3 J. D. Court, R. C. Brockhoff, and J. S. Hendricks, “Lawrence Livermore Pulsed Sphere Benchmark Analysis of MCNP ENDF/B-VI,” Los Alamos National Laboratory report, LA-12885 (1994).

4 D. J. Whalen et al.,”MCNP: Neutron Benchmark Problems,” Los Alamos National Laboratory report and errata, LA-12212 (1991).

5 S. C. Frankle, “Benchmark Problems for MCNP and the Data Libraries,” Los Alamos National Laboratory internal memorandum, X-6:SCF-95-92 (1995).

6 S.C. Frankle and R. E. MacFarlane, “Creation and Testing of An ENDF/B-VI Neutron Data Library (ENDF60) for use with MCNP,” proceedings of the Fifth International Conference on Nuclear Criticality Safety, LA-UR-95-2107 and LA-UR-95-3494, p. 6-148 (1995).

7 R. D. Mosteller, S. C. Frankle, and P. G. Young, “Data Testing of ENDF/B-VI with MCNP: Critical Experiments, Thermal-Reactor Lattices and Time-of-Flight Measurements,” to be published in Advances in Nuclear Science and Technology, LA-UR-96-2143 (1996).

8 “Cross Section Evaluation Working Group Benchmark Specifications,” Brookhaven National Laboratory report, BNL 19302 and ENDF-202 revised (1991).

9 “International Handbook of Evaluated Criticality Safety Benchmark Experiments,” NEA Nuclear Science Committee publication, NEA/NSC/DOC(95)03, Volumes I-VIII, (1996).

10 S. C. Frankle, “Summary Documentation for the ENDL92 Continuous-Energy Neutron Data Library (Release 1),” Los Alamos National Laboratory internal memorandum, XTM:SCF-96-327 and LA-UR-96-05 (1996).

11 C. E. Byers, “Cross Sections of Various Materials in the Godiva and Jezebel Critical Assemblies,” Nucl. Sci. Eng. **8**, p. 608 (1960).

12 L. Stewart, “Leakage Neutron Spectrum from a Bare Pu-239 Critical Assembly,” Nucl. Sci. Eng. **8**, p. 595 (1960).

13 G. E. Hanson and H. C. Paxton, “Re-evaluated Critical Specifications of Some Los Alamos Fast-Neutron Systems,” Los Alamos Scientific Laboratory report, LA-4208 (1969).

14 C. C. Cremer, R. E. Hunter, J. J. Berlijn, and D. R. Worlton, “Comparisons of Calculations with Integral Experiments for Plutonium and Uranium Critical Assemblies,” Los Alamos Scientific Laboratory report, LA-3529 (1969).

15 H. C. Paxton, “Los Alamos Critical-Mass Data,” Los Alamos National Laboratory report, LAMS-3067 (1964, rev. 1975).

16 C. C. Byers, J. J. Koelling, G. E. Hansen, D. R. Smith, and H. R. Dyer, “Critical Measurements of a Water-Reflected Enriched Uranium Sphere,” Trans. of American Nuclear Society 27, p. 412 (1977).

17 H. C. Paxton and N. L. Pruvost, “Critical Dimensions of Systems Containing ^{235}U, ^{239}Pu, and ^{233}U,” Los Alamos National Laboratory report, LA-10860 (1987 rev.)

18 J. K. Fox and L. W. Gilley, “Critical Parameters of Unreflected Arrays of Interacting Cylinders Containing Aqueous Solutions of ^{235}U,” Neutron Physics Division Annual Progress Report, Oak Ridge National Laboratory report, ORNL-2842 (1959).

19 H. F. Finn, N. L. Pruvost, O. C. Kolar, and G. A. Pierce, “Summary of Experimentally Determined Plutonium Array Critical Configurations,” Lawrence Livermore National Laboratory report, UCRL-51041 (1971).

20 C. G. Chezem and E. J. Lozito, “Investigation of the Criticality of Low-Enriched Uranium Cylinders,” Nucl. Sci. Eng. **33**, p. 139 (1968).

21 J. K. Fox, L. W. Gilley, and E. R. Rohrer, “Critical Mass Studies Part VIII: Aqueous Solutions of ^{233}U,” Oak Ridge National Laboratory report, ORNL-2143 (1959).

22 G. E. Hansen and H. C. Paxton, “A Critical Assembly of Uranium Enriched to 10% in Uranium-235,” Nucl. Sci. Eng. **72**, p. 230 (1979).

23 Alan Staub, D. R. Harris, and Mark Goldsmith, “Analysis of a Set of Critical Homogeneous U-H_2O Spheres,” Nucl. Sci. Eng. **34**, p. 263 (1968).

24 William H. Press et al., **Numerical Recipes, The Art of Scientific Computing (FORTRAN Version)**, Cambridge University Press, New York, 1989.
